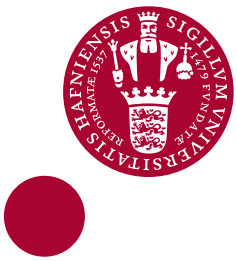

Enhancer and Transcription Factor Dynamics during Myeloid Differentiation Reveal an Early Differentiation Block in Cebpa null Progenitors

Pundhir, Sachin; Bratt Lauridsen, Felicia Kathrine; Schuster, Mikkel Bruhn; Jakobsen, Janus Schou; Ge, Ying; Schoof, Erwin Marten; Rapin, Nicolas Philippe Jean-Pierre; Waage, Johannes; Hasemann, Marie Sigurd; Porse, Bo Torben

Published in:
Cell Reports

DOI:
10.1016/j.celrep.2018.05.012

Publication date:
2018

Document version
Publisher's PDF, also known as Version of record

Cell Reports

Article

Enhancer and Transcription Factor Dynamics during Myeloid Differentiation Reveal an Early Differentiation Block in *Cebpa null* Progenitors

Graphical Abstract

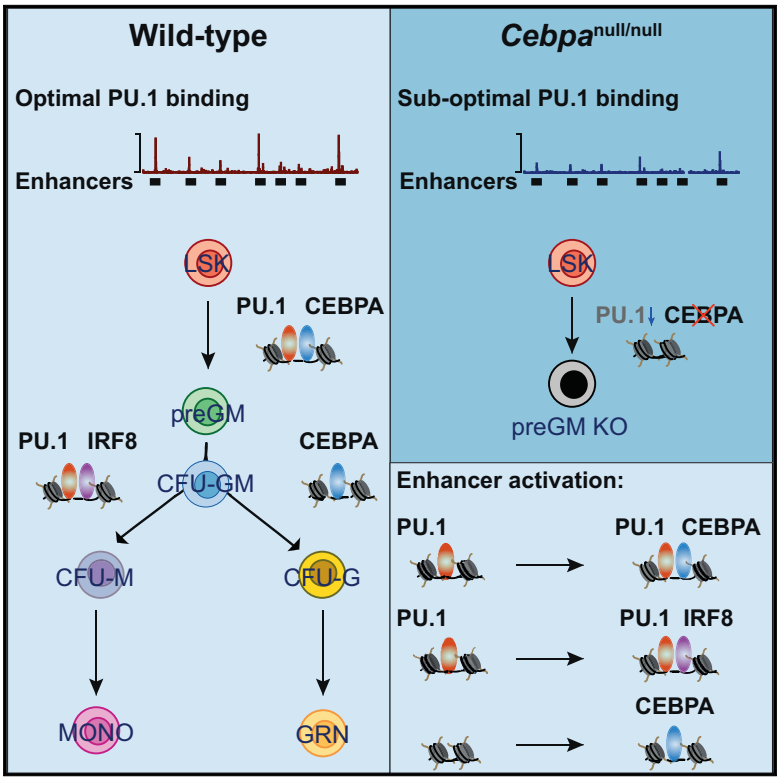

Highlights

- Characterization of the enhancer landscape during GM-lineage differentiation
- CEBPA controls PU.1 levels
- PU.1 binding to enhancers is diminished in *Cebpa null* GM progenitors
- Loss of CEBPA leads to a differentiation block upstream of CMPs/preGMs

Authors

Sachin Pundhir,
Felicia Kathrine Bratt Lauridsen,
Mikkel Bruhn Schuster, ...,
Johannes Waage,
Marie Sigurd Hasemann, Bo Torben Porse

Correspondence

bo.porse@finsenlab.dk

In Brief

Granulocytic-monocytic differentiation is governed by the PU.1 and CEBPA transcription factors (TFs). Here, Pundhir et al. use histone and TF ChIP-seq to demonstrate an unexpected role for CEBPA in controlling PU.1 function. They show that loss of CEBPA results in an early GM lineage differentiation block upstream of CMPs/preGMs.

Pundhir et al., 2018, Cell Reports *23*, 2744–2757
May 29, 2018
https://doi.org/10.1016/j.celrep.2018.05.012

CellPress

OPEN ACCESS
CellPress

Cell Reports
Article

Enhancer and Transcription Factor Dynamics during Myeloid Differentiation Reveal an Early Differentiation Block in *Cebpa null* Progenitors

Sachin Pundhir,[1,2,3,4,5] Felicia Kathrine Bratt Lauridsen,[1,2,3,5] Mikkel Bruhn Schuster,[1,2,3] Janus Schou Jakobsen,[1,2,3] Ying Ge,[1,2,3] Erwin Marten Schoof,[1,2,3] Nicolas Rapin,[1,2,3,4] Johannes Waage,[1,2,3,4] Marie Sigurd Hasemann,[1,2,3] and Bo Torben Porse[1,2,3,6,*]

[1]The Finsen Laboratory, Rigshospitalet, Faculty of Health Sciences, University of Copenhagen, Copenhagen, Denmark
[2]Biotech Research and Innovation Centre (BRIC), University of Copenhagen, Copenhagen, Denmark
[3]Novo Nordisk Foundation Center for Stem Cell Biology, DanStem, Faculty of Health Sciences, University of Copenhagen, Copenhagen, Denmark
[4]The Bioinformatics Centre, Department of Biology, Faculty of Natural Sciences, University of Copenhagen, Copenhagen, Denmark
[5]These authors contributed equally
[6]Lead Contact
*Correspondence: bo.porse@finsenlab.dk
https://doi.org/10.1016/j.celrep.2018.05.012

SUMMARY

Transcription factors PU.1 and CEBPA are required for the proper coordination of enhancer activity during granulocytic-monocytic (GM) lineage differentiation to form myeloid cells. However, precisely how these factors control the chronology of enhancer establishment during differentiation is not known. Through integrated analyses of enhancer dynamics, transcription factor binding, and proximal gene expression during successive stages of murine GM-lineage differentiation, we unravel the distinct kinetics by which PU.1 and CEBPA coordinate GM enhancer activity. We find no evidence of a pioneering function of PU.1 during late GM-lineage differentiation. Instead, we delineate a set of enhancers that gain accessibility in a CEBPA-dependent manner, suggesting a pioneering function of CEBPA. Analyses of *Cebpa null* bone marrow demonstrate that CEBPA controls PU.1 levels and, unexpectedly, that the loss of CEBPA results in an early differentiation block. Taken together, our data provide insights into how PU.1 and CEBPA functionally interact to drive GM-lineage differentiation.

INTRODUCTION

Myeloid cells such as macrophages and neutrophilic granulocytes constitute crucial components of the innate immune system. According to the classical models for the hierarchical architecture of the hematopoietic system, these cells develop from hematopoietic stem cells (HSCs) through a series of intermediate progenitor cells including common myeloid progenitors (CMPs)—or their near equivalents, the pre-granulocytemonocyte progenitors (preGMs)—and granulocytic-monocytic progenitors (GMPs). Specifically, these progenitors have been found to experience increasing degrees of lineage restriction as they progress along their path of differentiation (Orkin and Zon, 2008). The hierarchical organization of the hematopoietic system has been challenged by a number of studies that focus on single cells demonstrating extensive heterogeneity in progenitor populations previously thought to be homogeneous (Drissen et al., 2016; Paul et al., 2015). As an example, immunophenotypically defined CMPs harbor progenitors primed toward the megakaryocyte lineage and the monocytic lineage, as well as several granulocytic lineages (Paul et al., 2015). This suggests that lineage priming is an extensive phenomenon and that lineage fate decisions occur at earlier differentiation stages than was previously thought.

The dynamic patterns of gene expression during hematopoietic differentiation are governed by interactions between transcription factors (TFs) and proximal (promoter) and distal (enhancer) *cis*-regulatory elements (Boyle et al., 2008; Heintzman et al., 2009). Activities of distal enhancers are highly dynamic, as exemplified by global analyses of enhancer dynamics during hematopoietic differentiation (Lara-Astiaso et al., 2014; Luyten et al., 2014). More important, enhancer accessibility, as judged by nucleosome-deficient regions or H3K4me1/me2 marking, precedes gene expression.

PU.1 and CEBPA are key TFs during GM-lineage (myeloid) differentiation (Rosenbauer and Tenen, 2007). PU.1 is expressed throughout the hematopoietic hierarchy and is essential for the formation of CMPs/preGMs (Iwasaki et al., 2005; Scott et al., 1994). PU.1 binds to a vast number of enhancers and has been suggested to act as a so-called pioneering factor at a subset of these (Heinz et al., 2010). CEBPA is expressed during the latter stages of GM differentiation and is indispensable for the formation of GMPs (Zhang et al., 2004). Similar to PU.1, a role for CEBPA as a pioneering transcription factor has been suggested based in part on its ability to enhance the formation of induced pluripotent stem cells (iPSC) (Di Stefano et al., 2016; Ohlsson et al., 2016). However, the extent to which CEBPA plays a similar role during GM-lineage differentiation remains to be explored.

In line with their crucial importance during GM-lineage differentiation, the expression of both *Cebpa* and *Spi1* (encoding

CEBPA and PU.1, respectively) is tightly controlled. In humans, 14 different enhancers drive the expression of *CEBPA* in different tissues, with the −42 kb enhancer being responsible for the *CEBPA* expression in the GM-lineage (Avellino et al., 2016). Indeed, deletion of the corresponding and highly conserved −37 kb enhancer in the mouse efficiently ablates *Cebpa* expression in myeloid cells and leads to a phenotype that is essentially indistinguishable from that of knocking out *Cebpa* in the entire hematopoietic system (Avellino et al., 2016; Guo et al., 2016; Hasemann et al., 2014). *Spi1* expression is to a large extent controlled by a −14 kb enhancer, which in mice reduces the levels of PU.1 by 80% upon deletion (Rosenbauer et al., 2004). It is interesting that both PU.1 and CEBPA bind and activate this enhancer, demonstrating both autoregulation and CEBPA-dependent regulation of *Spi1* expression (Yeamans et al., 2007), although the importance of the latter has not been addressed in a proper *in vivo* setting.

Despite the evidence for extensive functional interplay between PU.1 and CEBPA, little is known of how these TFs work together to control the chronology of enhancer establishment during GM differentiation in a proper *in vivo* context. Here, we use a genome-wide chromatin immunoprecipitation-sequencing (ChIP-seq) approach to delineate the exact chronology of enhancer establishment during GM differentiation and its relation with the activity of PU.1 and CEBPA. We show that PU.1 predominantly binds at enhancers established during the early stages of differentiation and that late-established enhancers are gradually less dependent upon PU.1 binding. We observed instead that predominant CEBPA binding at late-established enhancers pointed toward a pioneering function of CEBPA at these elements. The distinct kinetics in the binding profiles of both PU.1 and CEBPA correlate with the enrichment of their respective sequence-binding motifs at enhancers. Analysis of *Cebpa*$^{-/-}$ (knockout [KO]) cells revealed a marked reduction in PU.1 binding at many enhancers, uncovering a surprising CEBPA dependency for binding of PU.1. Finally, we used these analyses to demonstrate that the loss of CEBPA leads to a GM differentiation block preceding preGMs.

RESULTS

Enhancer and Gene Expression Dynamics during GM-Lineage Differentiation

To characterize enhancer and gene expression dynamics along the GM-lineage, we generated genome-wide H3K4me1 and H3K27ac profiles from sorted LSK (Lin$^-$, Sca-1$^+$, ckit$^+$), preGM (constituting a subset of the CMPs; Lin$^-$, Sca-1$^-$, ckit$^+$, CD150$^-$, CD105$^-$), GMPs (Lin$^-$, Sca-1$^-$, ckit$^+$, CD150$^-$, FcgRII/III$^+$), neutrophilic granulocytes (GRN), and monocytes (MONO) representing five stages of murine GM differentiation (Figures 1A and S1A–S1C; Table S1). Since the main function of CEBPA is during granulocytic differentiation, we performed our primary analysis on four populations (LSK, preGM, GMP, and GRN). Additional analyses detailing the relative importance of PU.1 and CEBPA during GRN/MONO lineage choice is described in the latter part of this paper.

We used our recently developed peak-valley-peak (PVP) method, which relies on the local H3K4me1 distribution for the detection of active enhancers (Pundhir et al., 2016), to predict a total of 44,002 enhancers across the four populations (Figure S2A; Table S2), most of which (86%) were located distally (>500 bp) to transcription start sites (TSSs). Consistent with our previous observations, our PVP-predicted enhancers only display modest overlap (18%) with those derived from a classical read density-based approach (Lara-Astiaso et al., 2014; Pundhir et al., 2016). However, the PVP enhancers were associated with higher levels of accessibility (H3K4me1 and assay for transposase-accessible chromatin using sequencing [ATAC-seq]) and activity (H3K27ac), demonstrating that the H3K4me1 PVP pattern is efficient in capturing active enhancers (Figure S3A). Thus, our enhancer predictions provide an accurate map of the regulatory complexity and dynamics during GM differentiation, with enhancer regions showing distinct patterns of accessibility (Figures 1B [early], 1C [throughout], and 1D [late]).

Globally, we observed two major groups of enhancers that either maintain or lose H3K4me1 accessibility beyond the GMP stage (GRN-active and GRN-inactive) (Figure 2A). Within each group, we detected enhancer groups that gain and maintain H3K4me1 accessibility across distinct GM-lineage stages. These are exemplified by group 1 and group 5 enhancers, which are established in LSKs, whereas group 3 and group 7 enhancers are established at the GMP stage (Figure 2B). The accessibility profile of enhancers from each group correlated with a gradual gain in their activity as measured by H3K27ac levels and proximal gene expression, both of which followed similar profiles across the four stages (Figures 2C–2E and S3B).

Our enhancer classification was corroborated further by a distinct enrichment profile of previously reported myeloid enhancers in the GRN-active group and of stem cell enhancers in the GRN-inactive group (Lara-Astiaso et al., 2014) (Figure S3C). This observation suggests an active role for GRN-active enhancers in GM-lineage differentiation and a role for GRN-inactive enhancers during stem cell fate decisions. Indeed, we observed an enrichment of myeloid, lymphoid, and erythroid enhancers in the GRN-inactive group, consistent with the multipotent potential of LSK cells. However, we also note that even in this group, the frequency of myeloid-specific enhancers supersedes that of their lymphoid and erythroid counterparts, suggesting that priming toward the myeloid lineage is a key feature of the most immature blood cells. Finally, and consistent with their importance during myeloid differentiation, GRN-active enhancers are enriched for H3K27ac when compared to their GRN-inactive counterparts (Figures S2B–S2E). Taken together, we delineated enhancers into distinct groups that exert their regulatory functions across different stages of GM differentiation.

PU.1 and CEBPA Bind to a Large Fraction of GM Enhancers but Are Associated with Separate Groups of Enhancer Accessibility

To determine the TFs that are potentially associated with enhancer dynamics during GM differentiation, we compared the enrichments of *de novo* motifs in GRN-active and GRN-inactive enhancers. This demonstrates enrichment of the motifs that are associated with the myeloid master regulator CEBPA in GRN-active enhancers and with PU.1 in both GRN-inactive

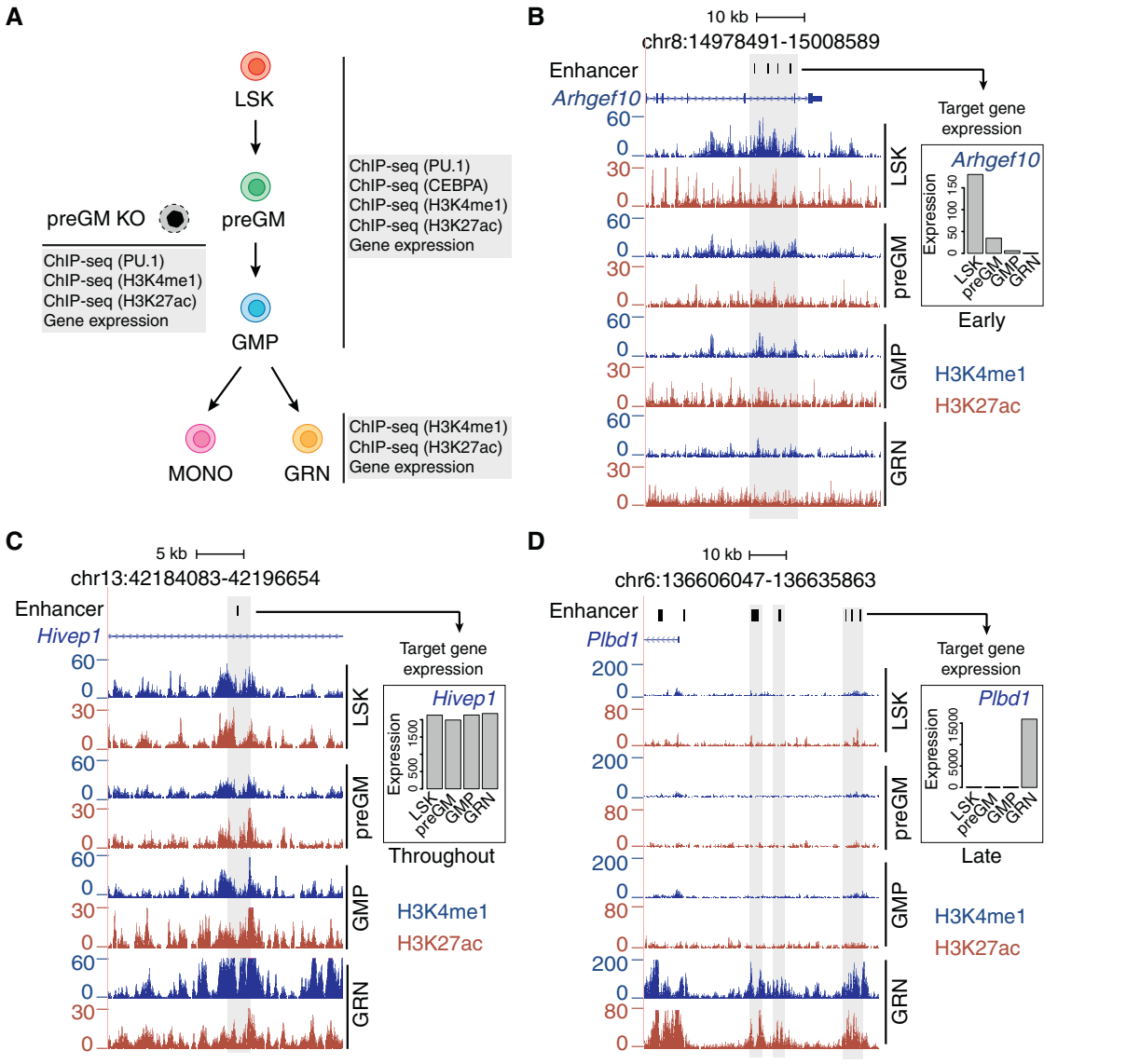

Figure 1. Experimental Outline

(A) Schematic diagram of the five GM differentiation stages profiled in the present study. Also shown are the datasets acquired from the different cell populations (gray boxes).

(B–D) Examples of differential enhancer behavior illustrated by enhancers that become accessible early (B), accessible throughout (C), or accessible at late differentiation stages (D). Shown are the normalized H3K4me1 and H3K27ac signal profiles (TPM) at these enhancers (gray boxes), as well as the gene expression profiles of the nearest gene associated with these enhancers (boxes).

See also Figure S1.

and GRN-active enhancers, which is consistent with the pan-hematopoietic importance of PU.1 (Figure S4A).

To elucidate further the roles of these factors during GM differentiation, we performed ChIP-seq in LSKs, preGMs, and GMPs and identified a total of 52,338 and 22,582 regions bound by PU.1 and CEBPA, respectively (Figure S4). Whereas 49% of PU.1-bound regions were identified in all populations, the number of CEBPA-bound regions increased gradually along the GM differentiation path. These findings are consistent with the expression patterns for these factors because CEBPA is upregulated as cells progress from LSKs to GMPs, while PU.1 is highly expressed at all stages. Well-known binding motifs for PU.1 and CEBPA were enriched in PU.1- and CEBPA-bound regions, respectively, along with a prominent enrichment of a PU.1-binding motif in CEBPA-bound regions. We find 31% of CEBPA-bound regions to be co-bound by PU.1 (Figure S4H) in GMPs, suggesting an extensive degree of cooperation between PU.1 and CEBPA.

Next, we categorized our enhancer set into those bound by either PU.1 or CEBPA, by both factors, or by others based on TF-binding profiles in GMPs (see Experimental Procedures). A

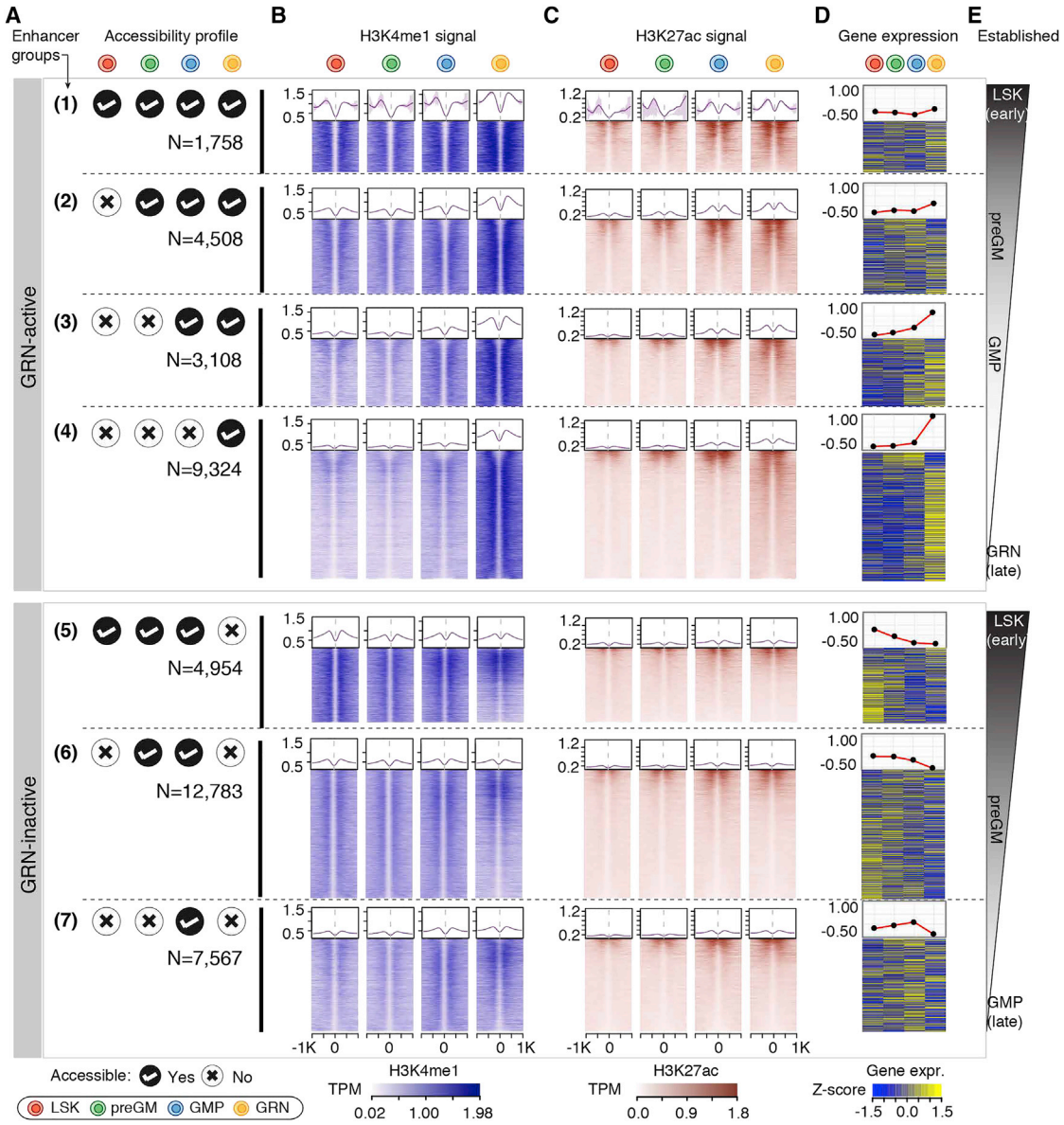

Figure 2. Enhancer and Gene Expression Dynamics during GM-Lineage Differentiation

(A) Classification of 44,002 enhancers into two major groups based on their activity in granulocyte (GRN-active and GRN-inactive), and further subclassified into four and three groups, respectively, based on their accessibility profile across the four GM-lineage differentiation stages (LSK, preGM, GMP, granulocytes). Filled and unfilled circles represent accessible and non-accessible enhancers as determined by their H3K4me1-derived PVP patterns.

(B) Normalized H3K4me1 signal (TPM) at midpoint-centered enhancers (rows, ±1,000 bp) across the four GM-lineage differentiation stages (columns; both as average and heatmap).

(C) The same as (B), but for H3K27ac.

(D) Scaled expression (*Z* score) of enhancer proximal genes across the four GM stages. Also shown is the median scaled signal at each stage above the heatmap.

(E) Schematic illustration of the early to late establishment of enhancers from the seven groups.

See also Figures S2 and S3.

substantial portion (36%) of these enhancers was bound by PU.1 and/or CEBPA and showed significantly higher levels of activity (H3K27ac; highest for co-bound) than the levels displayed by enhancers devoid of the two TFs (Figures 3A–3C). We used these data to determine the stages at which PU.1 and CEBPA exerted their main functions during GM-lineage differentiation, focusing on the GRN-active enhancers. Here, we observed a striking correlation between the timing of enhancer establishment and PU.1-binding levels (i.e., enhancers that were established in LSKs displayed higher levels of PU.1 in GMPs) (Figure 3E, group 1). Conversely, late-established enhancers displayed comparably lower levels of PU.1 (groups 2 and 3). These observations

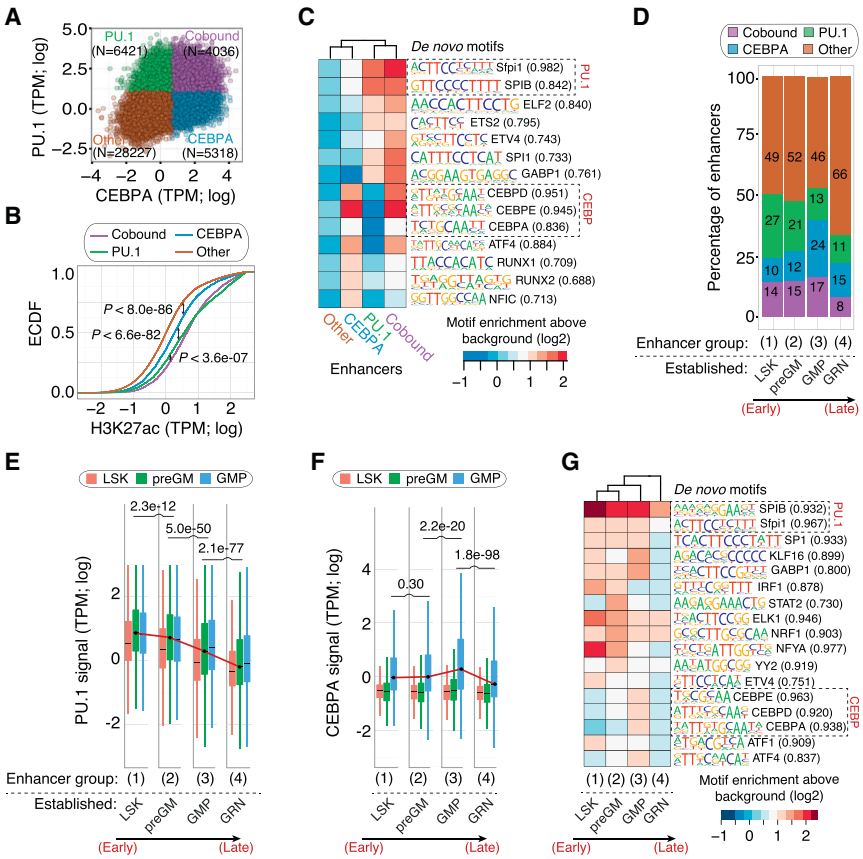

Figure 3. Differential Behavior of PU.1 and CEBPA at GM-Lineage Enhancers

(A) Enhancers (N = 44,002; bubbles) classified into four categories on the basis of normalized PU.1 (y axis) and CEBPA (x axis) signals.

(B) Density plot of the H3K27ac signal at four enhancer categories. ECDF, empirical cumulative distribution function (Kolmogorov-Smirnov test).

(C) Differentially enriched *de novo* sequence motifs at four enhancer categories. The top enriched and depleted motifs are shown along with their best-known motif match names.

(D) Fraction of enhancers from GRN-active groups bound by PU.1, CEBPA, both PU.1 and CEBPA, or other TFs (in GMPs).

(E) PU.1 binding signal (TPM) at enhancers belonging to the four GRN-active groups from LSKs to GMPs. p values (PU.1) represent the significance level at which the PU.1 signal (preGM) at enhancers from an earlier established group is higher than at enhancers from a later-established group (Wilcoxon rank-sum test).

(F) The same as (E), but for CEBPA binding. p values (CEBPA) represent the significance level at which CEBPA signal (GMP) at enhancers from two adjacent groups are different.

(G) Differential enrichment of *de novo* sequence motifs in the four GRN-active groups. The top enriched or depleted motifs are shown along with their best-known motif match name.

See also Figure S4.

correlated directly with the fraction of enhancers bound by PU.1 (Figure 3D). In contrast, CEBPA binding did not correlate with early enhancer establishment but was instead found mainly on group 3 enhancers that became established in GMPs (Figure 3F). Again, a higher fraction of these enhancers was associated with CEBPA binding compared to the other groups (Figure 3D). PU.1-binding motifs were consistently mainly enriched in early established enhancers, whereas CEBP motifs were preferably enriched in group 3 enhancers (Figure 3G).

Collectively, we have shown that PU.1 and CEBPA exert their main effects on enhancers that are established in LSKs and GMPs, respectively, and that the combined action of these two factors controls the activities of a substantial proportion of GM-lineage enhancers. Thus, our data uncover the underlying molecular basis for the critical roles of PU.1 and CEBPA in the formation of CMPs/preGMs and GMPs, respectively.

Loss of CEBPA Has a Strong Impact on PU.1 Binding

The current model of the PU.1/CEBPA interplay during late stages of GM differentiation holds that PU.1 facilitates the binding of CEBPA to numerous genomic loci by acting as a pioneering factor (Heinz et al., 2010). This model is consistent with both the expression patterns of PU.1 (early and maintained) and CEBPA (induced late) during GM differentiation and the extensive overlap of their binding profiles. However, given the early differentiation block in *Spi1*$^{-/-}$ myeloid progenitors, it has not been possible to test this model in a proper *in vivo* context, and it remains a formal possibility that CEBPA also controls PU.1 binding and levels.

Loss of CEBPA in murine bone marrow (BM) cells leads to a differentiation block upstream of GMPs (Hasemann et al., 2014; Zhang et al., 2004). To test the possibility that CEBPA may affect PU.1 function or levels, we isolated preGMs from *Cebpa*$^{-/-}$ mice (preGM-KO) and generated genome-wide binding profiles for PU.1, H3K4me1, and H3K27ac. The loss of CEBPA was associated with a significant loss of PU.1 peaks in preGM-KO (30,893 versus 44,813 in preGM-wild-type [WT]), suggesting that CEBPA controls the genome-wide association of PU.1 (Figure 4A). Moreover, we observed an overall reduction in PU.1 levels on the 44,002 GM-lineage enhancers when comparing preGM-KO to their WT counterpart (Figure 4B). Experiments in cell lines have shown that CEBPA binds and activates the −14 kb *Spi1* enhancer, which is a main driver of PU.1 transcription; this raises the possibility that the loss of CEBPA reduces the levels of PU.1 (Yeamans et al., 2007). We find that CEBPA binds this enhancer in LSK cells and that the loss of CEBPA is associated with a decrease in activity (H3K27ac; Figure 4C). We find reduced *Spi1* mRNA levels in preGM-KOs translating consistently into an approximate 2-fold reduction in PU.1 protein levels, as determined by quantitative mass spectrometry comparisons of WT and preGM-KOs (Figure 4D). Consistent with a previous report, loss of CEBPA leads to upregulation of the *Cebpg* mRNA and CEBPG protein (Figure 4D) (Alberich-Jordà et al., 2012). These findings clearly demonstrate that in addition

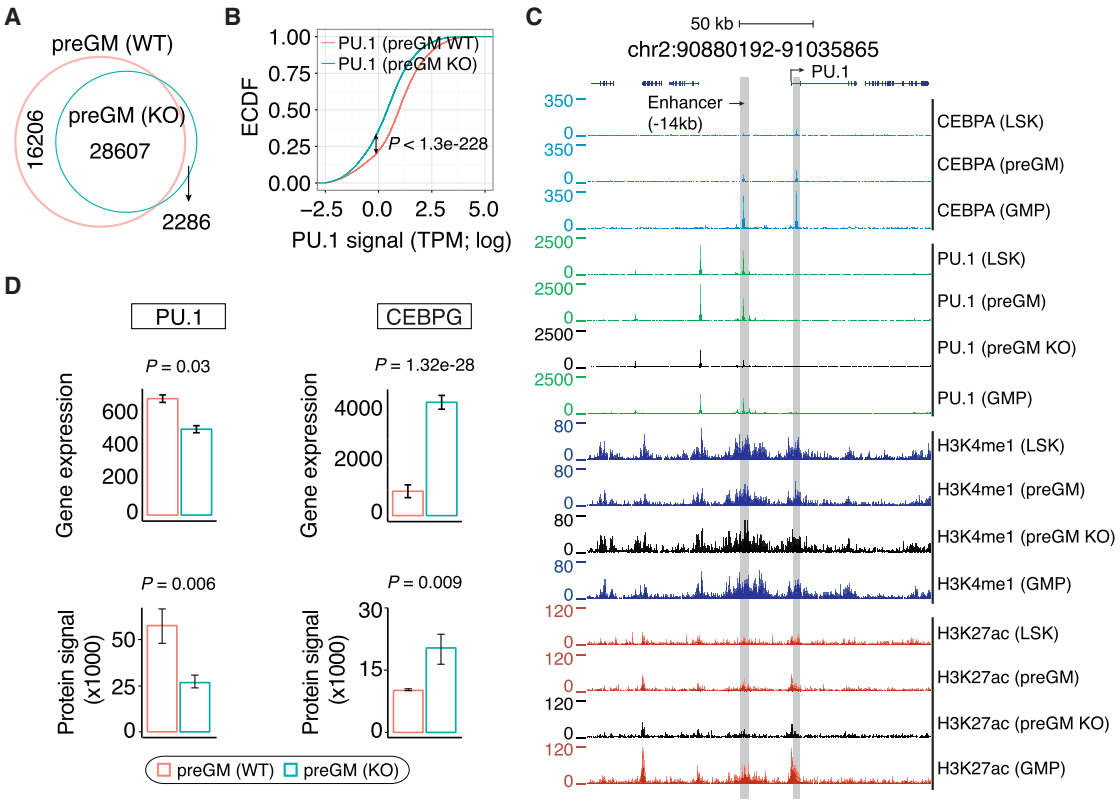

Figure 4. Loss of CEBPA Affects PU.1 Levels and Binding Properties

(A) Overlap between PU.1 peaks from WT and *Cebpa* KO preGMs.

(B) PU.1 density plots in WT and *Cebpa* KO preGMs (Kolmogorov-Smirnov test).

(C) University of California, Santa Cruz (UCSC) genome browser screenshot of PU.1 enhancers (gray). The −14 kb enhancer is indicated.

(D) *Spi1* and *Cebpg* expression (top) and corresponding protein levels (bottom) levels in WT and *Cebpa* KO preGMs (gene expression measured in DESeq2). Error bars represent the SD between the three replicates.

to the effect on CEBPA-bound enhancers, the loss of CEBPA also affects enhancers bound by PU.1 because of the overall reduction of PU.1 levels in preGM-KOs.

CEBPA Binds to GM-Lineage Enhancers in PU.1-Dependent and -Independent Manners

Our analyses so far have demonstrated a complex interplay between PU.1 and CEBPA during GM differentiation. Because loss of GMPs represents the main feature of CEBPA ablation, we decided to focus on changes in enhancer accessibility during the preGM to GMP transition.

To account for the recently reported heterogeneity in GMPs (Olsson et al., 2016), we further fractionated this population into colony-forming unit-granulocytes (CFU-Gs) and colony-forming unit-macrophages (CFU-Ms) (primed toward GRN and MONO production, respectively) and subjected these to TFs and histone profiling (Figures S1C and S1D). Focusing on GRN differentiation, we next ranked our 44,002 GM-lineage enhancers (from Figure 2) on the basis of their changes in H3K4me1 marks during the preGM to GMP transition. For each of the resulting 13 subclusters, we assessed the levels of PU.1, CEBPA, H3K4me1, H3K27ac, and gene expression in LSKs, preGMs, preGM-KOs, GMPs, and CFU-Gs (Figures 5A–5E). We further investigated the degree of change in these features during the transition from LSK to preGM, from preGM to GMP, and between WT and *Cebpa*$^{-/-}$ preGM (Figures 5F–5H). Enhancers belonging to cluster A gradually lose H3K4me1 from LSKs to GMPs, correlating with a reduction in H3K27ac and gene expression. Only a minor fraction of these enhancers is bound by PU.1 and/or CEBPA and mainly constitute GRN-inactive enhancers enriched for stem cell and non-GM-lineage enhancers (Figures 5I, 5J, and S3C). Cluster B is constituted by enhancers that either maintain (Bi) or moderately increase (Bii) their H3K4me1 levels as cells differentiate from LSKs to GMPs. A quarter of these enhancers (26%; 9,839 out of 37,519) are bound by PU.1 and this cluster also is characterized by the highest fraction of PU.1/CEBPA co-bound enhancers and by a transient gain of PU.1 binding from LSK to preGM. Most subcluster Bi enhancers lose PU.1 binding when differentiating onward to GMPs, whereas the Bii subcluster either maintains or further acquires PU.1 binding. Cluster B enhancers gain H3K27ac, but only the Bii subcluster enhancers activate gene expression in GMPs. Subcluster Bi enhancers overlap with stem and non-myeloid GRN-inactive enhancers, likely containing enhancers that are active in a variety of lineages (Figure 5J).

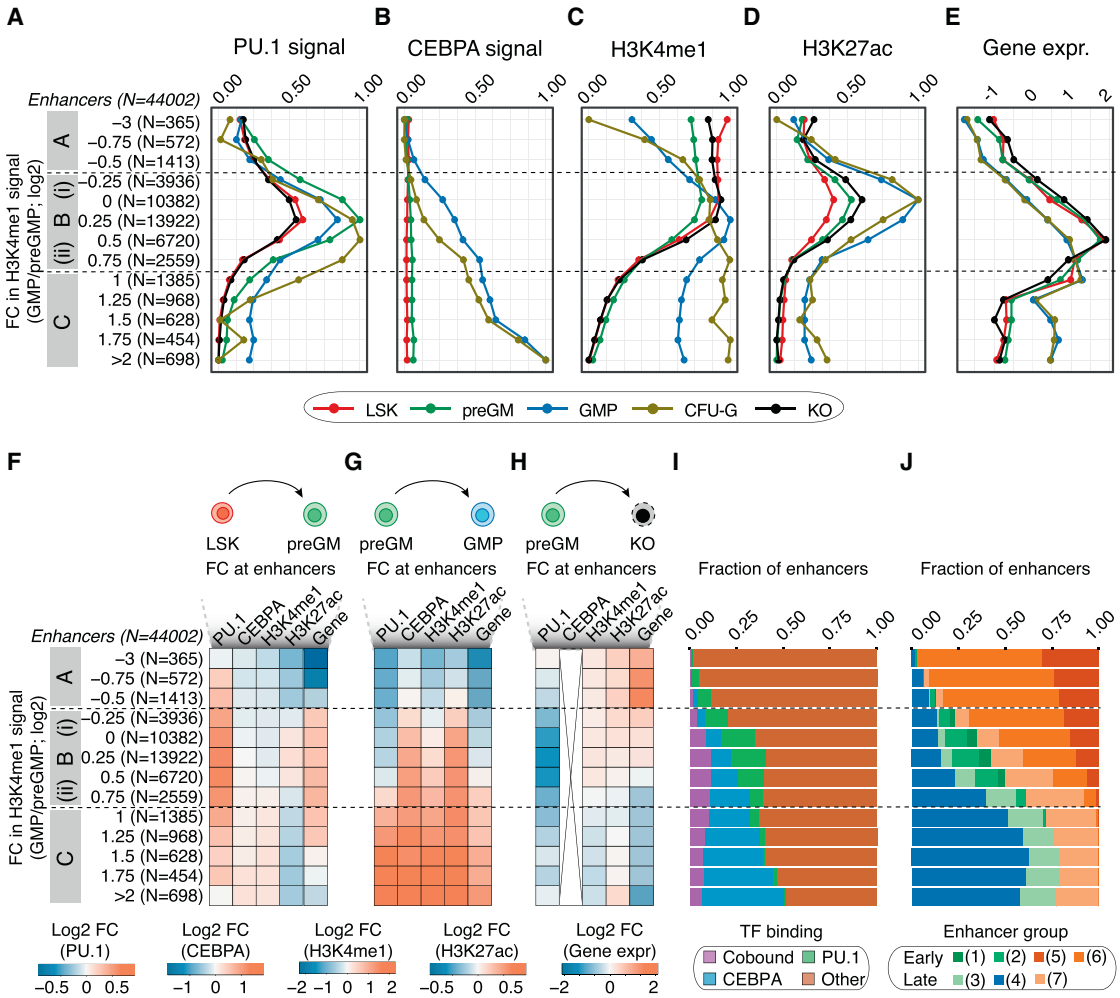

Figure 5. PU.1 and CEBPA Binding Profiles during GM-Lineage Differentiation

The 44,002 GM enhancers were ranked (N = 13) based on the fold change in H3K4me1 signal between the GMP and preGM stages (GMP/preGM).

(A) Mean PU.1 signal at GM enhancers from each cluster.

(B–E) The same as (A), but for CEBPA (B), H3K4me1 (C), and H3K27ac (D) and for the expression of the nearest associated gene (E).

(F) Median fold change in PU.1, CEBPA, H3K4me1, and H3K27ac levels at enhancers from each cluster during the LSK to preGM transition along with gene expression fold changes of the nearest associated gene.

(G and H) The same as (F), but for the preGM to GMP transition (G) and between WT and *Cebpa* KO preGMs (H).

(I) Fraction of enhancers bound by PU.1, CEBPA, both PU.1 and CEBPA, or other TFs.

(J) Differential enrichment of seven enhancer groups (from Figure 2) at enhancer clusters A, B, and C.

See also Figures S5 and S6.

It is interesting that the transcription of cluster B enhancer-driven genes is induced mainly transiently, suggesting that they may be important for promoting preGM formation. Of note, the gain of H3K27ac on subcluster Bii enhancers correlates with CEBPA binding, suggesting that CEBPA activates enhancers already marked by PU.1. However, because these enhancers are bound by PU.1 already in LSKs, any potential pioneering function of PU.1 will have to occur at earlier developmental stages. Finally, cluster C contains enhancers that are established mainly in GMPs. These enhancers are characterized further by low levels of PU.1 in preGM and acquire CEBPA binding in GMPs, followed by an increase in PU.1 levels (Figures S5A and S5B). This correlates strictly with the acquisition of H3K27ac and activation of gene expression. Indeed, cluster C enhancers are highly enriched for CEBPA, suggesting that CEBPA is able to assess closed chromatin in the absence of PU.1. The behavior of clusters A–C enhancers are further stratified based on their PU.1 and CEBPA binding status (Figure S6).

To gain further insight into the enhancers controlled by CEBPA at the preGM to GMP transition we took advantage of our gene expression data to define a group of CEBPA-dependent genes (up during the preGMP to GMP transition and down in preGM-KOs) and CEBPA-independent genes (down during the preGMP to GMP transition and up in preGM-KOs compared to preGMs; Figure S5C). CEBPA-dependent genes are markedly enriched for genes involved in GM-specific gene programs and are

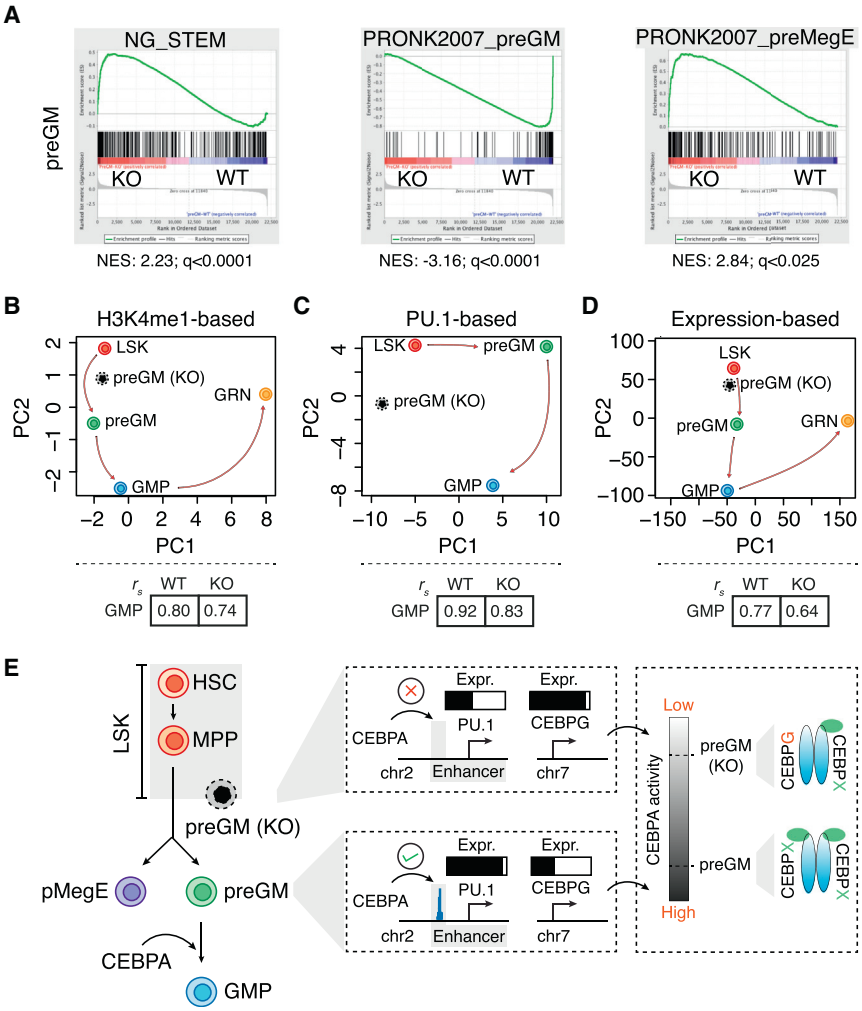

Figure 6. Loss of CEBPA Leads to a Differentiation Block Upstream of the preGM

(A) GSEA of preGMs derived from WT and *Cebpa* KO BM.

(B) Principal component analysis (PCA) analysis of H3K4me1 data on GM-lineage enhancers.

(C) The same as (B), but for PU.1 binding data.

(D) The same as (B), but for gene expression. Also shown below each PCA plot is the correlation between signal values (H3K4me1, PU.1 or expression) in GMP and preGM WT or KO.

(E) Model illustrating the differentiation block in *Cebpa* KO BM and its impact on *Spi1* and *Cebpg* expression. Loss of CEBPA will lead to increased CEBPG levels, which in turn result in a lowering of overall CEBP activity. We hypothesize that the combined reduction in PU.1 and CEBPA activity is responsible for the early differentiation block in *Cebpa* KO BM.

prominently controlled by cluster C enhancers (Figures S5D and S5E). Conversely, CEBPA-independent genes are enriched for T cell development pathways and are mainly controlled by cluster A enhancers (Figures S5D and S5E). Finally, to directly demonstrate a pioneering function of CEBPA during the preGM to GMP transition, we re-expressed CEBPA in preGM-KO cells to drive GM differentiation (Figures S5F–S5H). It is striking that CEBPA binding to six of eight tested CEBPA-dependent enhancers (cluster C) was associated with a marked increase in chromatin accessibility as detected by ATAC-qPCR (Figures S5I and S5J). Conversely, a collection of six cluster A or B enhancers was unaffected by CEBPA expression. These results demonstrate that CEBPA engages with closed chromatin and facilitate the establishment of a class of signature GRN enhancers during the preGM to GMP transition.

Collectively, our analyses demonstrate that differentiation along the GM path is associated with distinct patterns of enhancer behavior involving (1) cluster A enhancers that shut down mainly in a PU.1- and CEBPA-independent manner; (2) the heterogeneous cluster B enhancers, which exhibit dynamic patterns of PU.1 occupancy; and (3) the highly CEBPA-dependent cluster C enhancers, which are activated at the GMP stage, in part through the pioneering function of CEBPA, and positively regulate the transcriptional program required for GM differentiation.

CEBPA Loss Blocks GM Differentiation Upstream of the preGM Stage

Previous studies, including our own, have demonstrated that *Cebpa*$^{-/-}$ mice exhibit a differentiation block upstream of the GMP (Hasemann et al., 2014; Mancini et al., 2012; Zhang et al., 2004). The identity of the upstream progenitor depends on the immunophenotyping strategies used in these particular studies, and both CMPs and preGMs have been shown to accumulate in the absence of CEBPA. However, the immunophenotypes of CMPs and preGMs only differ from the immunophenotype of upstream LSK cells by the loss of Sca-1 expression, thus rendering the definition of these progenitors sensitive to the expression kinetics of this marker. Moreover, because the functional definition of *Cebpa*$^{-/-}$ progenitors is prohibited by the inability of these cells to sustain GM output, we decided to take a more global approach to characterizing preGM-KO cells. The changes across our ranked enhancers (clusters A–C) comparing KO to WT preGMs were almost the complete opposite of the changes occurring at the LSK to preGM transition (Figure 5H, compare to Figure 5F), thereby placing immunophenically defined preGM-KOs near the LSK compartment.

Gene set enrichment analysis (GSEA) demonstrated consistently that preGM-KOs were enriched for the expression of a pre-megakaryocyte erythrocyte progenitors (preMegEs) signature and depleted of the expression of a preGM signature relative to their WT counterparts (Figure 6A). This, along with the observed increased expression of a stem cell signature in preGM-KOs, places this population upstream of its WT

counterpart (Figure 6A). Because our analysis of enhancer usage demonstrates extensive dynamics of PU.1 binding and H3K4me1 levels during differentiation along the GM-lineage, we next used principal-component analysis of these features as well as of global gene expression to further assign the differentiation block of *Cebpa*$^{-/-}$ GM progenitors. All three features placed preGM-KOs upstream of preGM-WTs and immediately downstream of LSKs (Figures 6B–6D). Overall, these findings suggest that loss of CEBPA results in the inability of LSKs to progress beyond the point of downregulation of Sca-1 expression, thereby moving the CEBPA restriction point to a position well before the preGM population (Figure 6E).

The Distinct Chromatin Landscapes of Granulocytic and Monocytic Progenitors Prime Their Differentiation toward Mature Populations

CEBPA and PU.1 are known to drive differentiation toward the granulocytic and monocytic lineages, respectively, but how this differential behavior is coordinated and how it relates to the recently described functional heterogeneity within the GMP population remains unanswered. To address these questions, we first classified 37,221 enhancers as common or specific to GRN and MONO lineages based on the ratio of their H3K4me1 levels in granulocyte and monocyte populations, respectively (Figure S7A; Experimental Procedures). Next, we assessed the activity and TF occupancy at these enhancers in their corresponding upstream progenitors. In support of a priming model, we find that both GRN- and MONO-specific enhancers displayed higher levels of activity (H3K27ac) and proximal gene expression already in their respective progenitor populations (CFU-Gs and CFU-Ms) and that their activity gradually increased as cells differentiate into granulocytes or monocytes (Figure 7A). Furthermore, PU.1 binding was relatively higher at MONO- compared to GRN-specific enhancers already in preGMs, whereas a weak but opposite trend was observed for CEBPA (Figure 7A). These findings are corroborated further by the observed enrichment of CEBPA and PU.1 sequence motifs in GRN- and MONO-specific enhancers, respectively (Figure 7D).

GRN-specific enhancers are highly enriched for the previously defined CEBPA-dependent cluster C enhancers (Figure 7B). Likewise, these enhancers are activated (H3K27ac) concomitantly with the acquisition of CEBPA binding in CFU-Gs and are associated with an increase in target gene expression (Figures 7A–7C). Although CEBPA binding to GRN-specific enhancers also increases in CFU-Ms, this increase is much less pronounced and is not accompanied by increases in H3K27ac and gene expression levels (Figure 7A).

For the MONO-specific enhancers, CEBPA binding remains low while PU.1 occupancy increases, albeit to the same levels in both CFU-Gs and CFU-Ms. The latter observation suggests that other TFs are instrumental for monocyte differentiation in line with the well-established role for interferon regulatory factor (IRF) family members such as IRF8 (Figures 7A, S7B, and S7C) (Becker et al., 2012). Indeed, several IRF motifs are selectively enriched at MONO-specific enhancers, and IRF8 is the most upregulated factor in CFU-Ms relative to CFU-Gs (Figures 7D and 7E). Finally, a major fraction of enhancers (N = 22,332) was common to both granulocytes and monocytes. These enhancers displayed high levels of H3K27ac and gene expression in preGM, which remained constant as the cells differentiated toward CFU-Gs and CFU-Ms. While PU.1 occupancy at these enhancers decreased as preGMs differentiate into CFU-Gs or CFU-Ms (Figure 7A), CEBPA binding increased, albeit more profoundly in CFU-Gs (Figure 7A). The kinetics of PU.1 and CEBPA are similar to our previous observation for PU.1-driven enhancers (cluster B in Figure 5) that govern the differentiation from LSKs to preGMs. Indeed, we found a significant overlap between cluster B enhancers with this common group of GM enhancers (Figure 7B).

Finally, to discern the transcriptional program regulated by GRN- and MONO-specific enhancers, we defined 376 (CFU-G) and 457 (CFU-M) genes that are differentially expressed between the CFU-G and CFU-M populations (Figures 7E and S7D). We observed an enrichment of functional categories that are crucial for the immune function of each of the two lineages (Figure S7E). We also detected a relative increase in the expression of cell-cycle genes in CFU-Ms compared to that of CFU-Gs (Figures 7E and S7E). We hypothesize that the selective repression of cell-cycle genes in CFU-Gs is associated with the increased expression of CEBPA in this compartment, which would be consistent with its recognized function as a negative regulator of proliferation (Johansen et al., 2001; Porse et al., 2001).

In conclusion, MONO- and GRN-specific enhancers are established as preGMs differentiate toward CFU-Ms and CFU-Gs, respectively, and are differentially occupied by PU.1 and CEBPA during GM-lineage differentiation (Figure 7F).

DISCUSSION

Defining how gene regulatory networks serve to shape biological properties is key to understanding how cells progress from immature stem and progenitor cells into their mature progeny. Differentiation processes are governed by the actions of TFs, some of which exhibit highly lineage-restricted expression patterns. Within the hematopoietic system, CEBPA is expressed almost exclusively in the GM branch of the hematopoietic hierarchy and is ultimately required for the development of mature myeloid cells, but the underlying mechanisms for this requirement have remained elusive. By integrated analysis of enhancer dynamics, TF binding, and proximal gene expression during GM-lineage differentiation in the context of a normal and a *Cebpa*$^{-/-}$ hematopoietic system, we showed an extensive functional interplay between CEBPA and PU.1 in driving GM-lineage differentiation. Moreover, our analyses also demonstrate that the loss of CEBPA leads to a differentiation block at an earlier stage than previously reported. Thus, our work yields insights into how TFs functionally interact to drive differentiation along the GM-lineage.

Enhancer Dynamics during Differentiation along the GM-Lineage

Using our recently developed PVP approach for the analysis of histone modifications, we defined the enhancer landscapes during differentiation from multipotent progenitors (LSKs) to mature neutrophilic granulocytes. A large fraction of identified

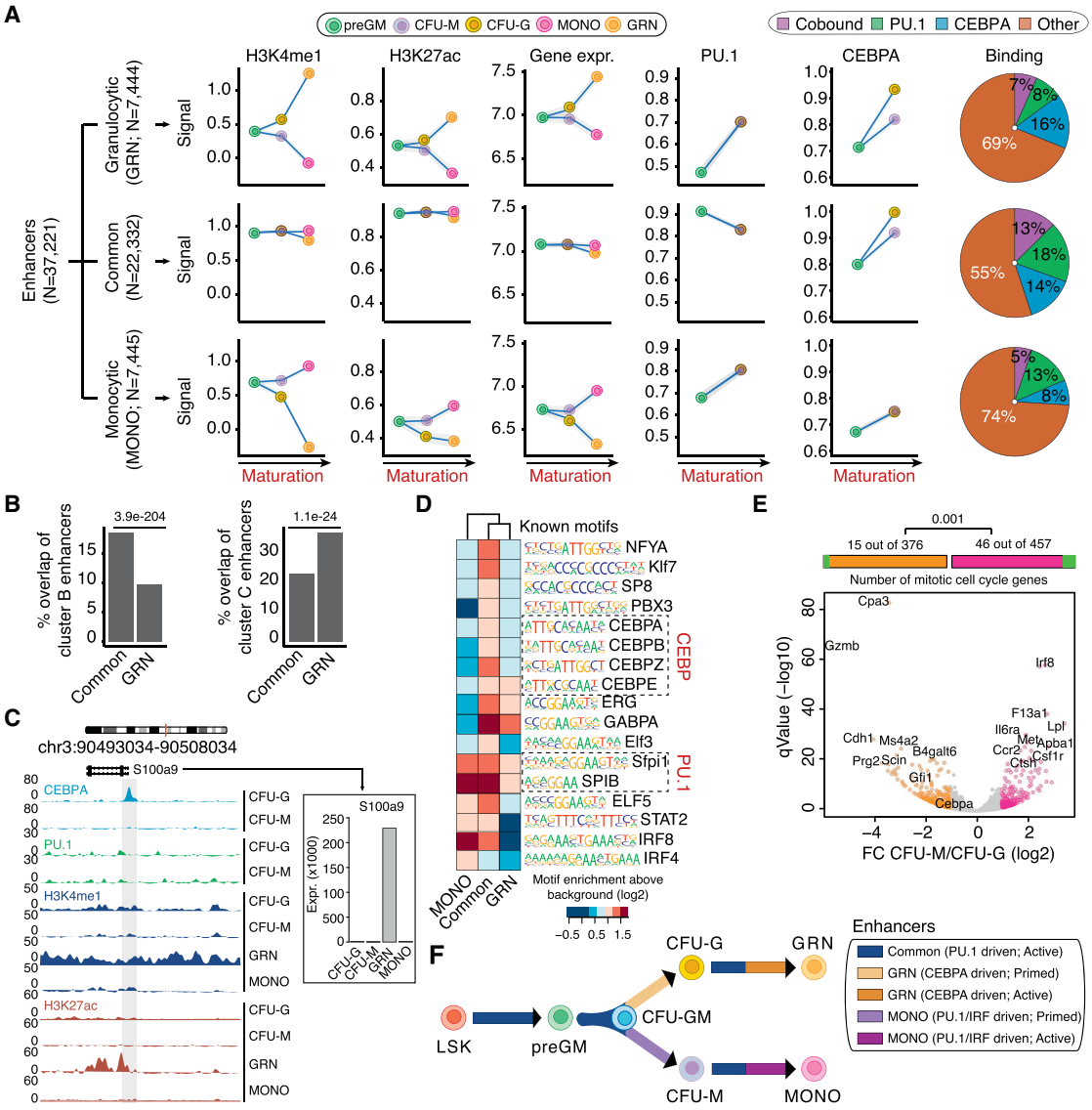

Figure 7. Monocytic Enhancers Are Distinct from Granulocytic Enhancers in Terms of Their Transcription Factor Environment and Target Genes

(A) Enhancers classified on the basis of their activity in granulocytic, monocytic, or both lineages. The dynamics of H3K4me1, H3K27ac, proximal gene expression, PU.1, and CEBPA binding levels (quantile normalized) during differentiation of preGMs toward granulocytes or monocytes via the CFU-G or CFU-M intermediates, respectively. Also shown is the fraction of enhancers from the three classes that are bound by PU.1, CEBPA, or both TFs in the GMP stage.

(B) Percentage of group C and B enhancers from Figure 5 that overlaps with common and granulocytic enhancers (Fisher's exact test).

(C) A representative example of a CEBPA-bound enhancer active specifically in the granulocytic lineage.

(D) Differentially enriched sequence motifs in the three enhancer classes. The top enriched and depleted motifs are shown.

(E) Volcano plot for 833 differentially expressed (DE) genes between CFU-G and CFU-M. Names of selected DE genes are shown, along with the fraction of DE cell-cycle genes between the two populations.

(F) Model illustrating the differential activity profile of PU.1 and CEBPA-dependent enhancers during GM differentiation. The CFU-GM population is indicated for the sake of completion, although it was not assayed here.

See also Figure S7.

enhancers was accessible already at the LSK stage and became either more accessible (GRN-active) or was shut down (GRN-inactive) during GM differentiation, demonstrating both a high degree of enhancer dynamics and a high level of lineage priming in immature populations (Lara-Astiaso et al., 2014; Paul et al., 2015). Indeed, enhancers that became closed in mature cells were assigned mainly to non-GM-lineage genes and genes associated with stem cell functions.

De novo motif analysis identified PU.1 and CEBPA as potential key TFs at GRN-active enhancers. Consistent with this notion,

PU.1 and CEBPA bound pervasively to GM-lineage enhancers, and enhancers bound by either or both of these factors were enriched for enhancer activity. PU.1 preferred enhancers that were accessible at earlier stages, likely reflecting its role as a pan-hematopoietic master TF (Wilson et al., 2010). In contrast, CEBPA bound mainly to late-accessible enhancers, which is consistent with its expression pattern and its importance in inducing the expression of genes involved in granulocyte function and development. Finally, by additional subfractionation of GMPs into CFU-Ms and CFU-Gs, we were able to provide evidence for the selective importance of CEBPA in the latter population, which is consistent with the view of CEBPA as the key TF during granulocytic differentiation. Overall, these analyses reveal the underlying molecular basis for the importance of both PU.1 and CEBPA in setting up gene regulatory programs during GM-lineage differentiation.

Several Layers of Functional Interaction between PU.1 and CEBPA

PU.1 has been reported to serve as a pioneering factor during GM-lineage differentiation, facilitating H3K4me1-driven enhancer formation and subsequent recruitment of TFs, including CEBPs (Heinz et al., 2010). Although these data clearly demonstrate the ability of PU.1 to bind and remodel closed chromatin, the fact that they were generated by re-expression of a PU.1-ER fusion protein in a PU.1 *null* context does not allow us to assess the extent to which this occurs during normal GM-lineage differentiation. In the present work, we observed little evidence for PU.1 binding to closed chromatin, most likely reflecting the fact that a vast amount of hematopoietic enhancers are marked by PU.1 already in HSCs (Wilson et al., 2010). However, our data do not exclude a pioneering function for PU.1 at early stages such as during HSC specification or in other hematopoietic lineages.

Cluster C enhancers constitute a group of enhancers that remains inaccessible in the absence of CEBPA. In contrast to PU.1, CEBPA binding clearly correlates with the opening and activation of these enhancers, and re-expression of CEBPA in cultured *Cebpa null* progenitors was associated with enhancer opening concomitant with CEBPA binding. These findings strongly suggest that CEBPA acts as a pioneering factor on selected enhancers, perhaps via its switch/sucrose nonfermentable (SWI/SNF) domain, which has been shown to be important for enhancer binding in adipocyte differentiation (Madsen et al., 2014).

PU.1 and CEBPA exhibit extensive co-binding at GM-lineage enhancers. A large degree of CEBPA binding occurs at enhancers already bound by PU.1, but also we detect examples of enhancers in which PU.1 binding is dependent on CEBPA. These examples include co-bound enhancers in which PU.1 binding follows CEBPA occupancy (Figures 5, S5A, and S5B). This dependency may reflect the lower expression of PU.1 in *Cebpa*$^{-/-}$ cells, where we observe an overall reduction in PU.1 binding. The reduction in PU.1 expression could be traced back to the −14 kb *Sfi1* enhancer, where CEBPA binding was detected in LSK cells. Collectively, our data suggest not only that CEBPA binds to chromatin in PU.1-dependent and -independent manners but also that CEBPA is important for maintaining appropriate levels of PU.1. Hence, these findings extend the current view on the PU.1/CEBPA interplay during GM-lineage differentiation toward a more active role for CEBPA.

Loss of CEBPA Leads to an Early Block in GM Differentiation

Previous studies have placed the CEBPA-mediated differentiation block during GM differentiation immediately upstream of the GMP (Hasemann et al., 2014; Mancini et al., 2012; Zhang et al., 2004). This was inferred from the accumulation of the immediate upstream population (i.e., preGM or CMP), depending on the specific immunophenotyping strategy. However, preGMs and CMPs differ from the broad LSK population only through their lack of Sca-1 expression. Using gene expression data and H3K4me1 and PU.1 ChIP-seq data, we showed that *Cebpa*$^{-/-}$ preGMs mapped closely to LSKs, suggesting that the loss of *Cebpa* leads to a differentiation block upstream of the preGM at a stage immediately after downregulation of Sca-1 expression (Figure 6E). Previous studies have shown that loss or functional inactivation of CEBPA in various settings frequently is associated with the aberrant expression of erythroid and lymphoid gene expression signatures (Bereshchenko et al., 2009; Mancini et al., 2012; Schuster et al., 2013; Wouters et al., 2007). Consistently, preGM/CMP expressing no or functionally compromised CEBPA shows an increased potential toward non-GM-lineages. Moreover, in a leukemic setting, epigenetic silencing of *CEBPA* sustains the production of leukemic blasts with both T cell and GM characteristics, whereas BCR-ABL, normally associated with GM leukemias, promotes the formation of erythroleukemias when overexpressed in *Cebpa*$^{-/-}$ progenitors (Figueroa et al., 2009; Wagner et al., 2006; Wouters et al., 2007). Whereas these non-GM-lineage characteristics of *Cebpa*$^{-/-}$ progenitors have been interpreted to reflect the loss of lineage fidelity imposed by the absence of *Cebpa*, they may as well reflect a less differentiated phenotype of *Cebpa*$^{-/-}$ progenitors, which is consistent with the model supported by our data. Indeed, this interpretation is supported further by single-cell RNA sequencing (scRNA-seq) analysis of Lin^{-},Sca-1^{-},c-kit^{+} progenitors, where loss of *Cebpa* leads to the formation of a transcriptional cluster characterized by the co-expression of GM, erythroid, and lymphoid genes (Paul et al., 2015). We hypothesize that this cluster represents a subset of our *Cebpa*$^{-/-}$ preGMs.

Reports have highlighted the importance of CEBPA as a transcriptional repressor in LSK cells, promoting the repression of target genes such as *Sox4* and *Cebpg* (Alberich-Jordà et al., 2012; Zhang et al., 2013). Consequently, the loss of CEBPA leads to increased expression of these factors and the GM differentiation block was rescued by short hairpin RNA (shRNA)-mediated knock down of either of these factors. Whereas the underlying mechanism of SOX4 remains unclear, CEBPG, which lacks a transactivation domain, was shown to control overall CEBP activity in *Cebpa*$^{-/-}$ progenitors through its ability to repress both the levels and transactivation potential of CEBPB (Alberich-Jordà et al., 2012). The latter presumably occurs through the leucine zipper-mediated heterodimerization with CEBPB, a factor that is able to functionally substitute for CEBPA, as evidenced by the lack of any overt hematopoietic phenotypes of mice expressing *Cebpb* from the *Cebpa* locus (Jones et al., 2002).

Thus, the loss of CEBPA leads to an additional lowering of overall CEBP activity below a threshold that is able to sustain GM-lineage differentiation (Figure 6E).

Although the expression of single genes such as *Cebpg* may explain the *Cebpa*$^{-/-}$ phenotype, it is equally important to consider the global impact of CEBPA during GM-lineage differentiation. Differentiation from LSKs to preGM requires the coordinated down- and upregulation (Figures S5C and S5D) of numerous genes, and our enhancer analysis demonstrates that a large proportion of these are bound by PU.1 and/or CEBPA (Figure 5I). Given that PU.1 expression is lowered in *Cebpa*$^{-/-}$ progenitors, presumably through the action of CEBPA on the −14 kb *Sfi1* enhancer, and because PU.1 is bound to a vast amount of GM enhancers, we consider it likely that the reduced PU.1 level in the context of *Cebpa*$^{-/-}$ progenitors is important at the LSK to preGM transition. In support of this, the loss of PU.1 leads to the complete absence of CMPs, whereas heterozygous animals exhibit a mild reduction in CMPs (Iwasaki et al., 2005). In light of the extensive functional interplay between PU.1 and CEBPA at GM enhancers, we hypothesize that the absence of CEBPA, which is further exacerbated by the aforementioned CEBPG-mediated lowering of CEBP activity, sensitizes LSK cells to a reduction in PU.1 level, ultimately resulting in a differentiation block upstream of the preGM (Figure 6E).

EXPERIMENTAL PROCEDURES

Mouse Work

Animals were housed according to institutional guidelines at the University of Copenhagen. The conditional *Cebpa null* line and the *Mx1Cre* driver lines were intercrossed to generate *Cebpa*$^{fl/fl}$ and *Cebpa*$^{fl/fl}$*;Mx1Cre* and genotyped as described previously (Hasemann et al., 2014; Kühn et al., 1995; Lee et al., 1997). Female mice 10–12 weeks old were subjected to three injections (days 0, 2, and 4) with 200 μL polyinosinic-polycytidylic acid (pIpC; 1.5 mg/mL in PBS; GE Healthcare) as described previously (Hasemann et al., 2014). Mice were analyzed at day 18 after the first pIpC injection. Mouse work was performed according to institutional guidelines and by permission of the Danish Animal Experiments Inspectorate.

RNA-Seq

Total RNA was extracted from LSK, preGMs, GMP, CFU-G, CFU-M, granulocytes, and monocytes in biological triplicates, using the RNeasy Micro Kit (QIAGEN). RNA was processed for double-stranded cDNA synthesis using the Ovation RNA-Seq System V2 (NuGEN). The sheared cDNA (fragment size from 150 to 550 bp) was subjected subsequently to library preparation using the Ovation Ultralow System V2 (NuGEN). The indexed cDNA libraries were pooled in equimolar ratios and subjected to 75-cycles sequencing on the NextSeq 500 System (Illumina).

ChIP-Seq

For histone marks and TF (PU.1 and CEBPA) we used 100,000-250,00 and 500,000 cells, respectively, per experiment. For neutrophils, we used 500,000–1,000,000 cells, given their availability. ChIP was performed as described previously (Hasemann et al., 2014), except that cell lysates from neutrophils were supplied with 5 nM NaF and 0.1 mM Na_3VO_4. The following antibodies were used: PU.1 (Sc-352, Santa Cruz), CEBPA (14AA, Santa Cruz), H3K4me1 (ab8895, Abcam), H3K27ac (ab4729, Abcam), and immunoglobulin G (IgG) (Sc-2027, Santa Cruz). Washing procedures were optimized for the individual antibodies as follows: PU.1: 2x rinse and 1x wash in radioimmunoprecipitation assay (RIPA; 140 mM NaCl, 10 mM Tris-HCl, 1 mM EDTA, 1% Triton X-100, 0.1% SDS, 0.1% sodium deoxycholate, 1 mM PMSF), followed by 4x wash in RIPA with 0.5 M NaCl, 1x wash in LiCl buffer (250 mM LiCl, 10 mM Tris-HCl, 1 mM EDTA, 0.5% NP-40, and 0.1% sodium deoxycholate), and 2x wash in TE buffer (10 mM Tris-HCl, 1 mM EDTA). H3K4me1/H3K27ac: 2x rinse in RIPA, followed by 4x wash in RIPA, 1x wash in LiCl buffer, and 2x wash in TE buffer. CEBPA and IgG: As described by Hasemann et al. (2014). Nucleotide sequences corresponding to the two replicates from each cell population were mapped to mouse genome (mm9) using Bowtie 2 (default parameters) (Langmead and Salzberg, 2012).

Prediction of Active Enhancer Regions

We used PARE (version 0.01), a computational method that captures H3K4me1-defined open chromatin regions, to predict active enhancer regions in the four GM differentiation stages (LSK, preGM, GMP, and granulocytes) (Table S2) (Pundhir et al., 2016). We selected active enhancer regions that were reproducible in both replicates at a false discovery rate (FDR) of <0.05. This gave us a binary matrix of enhancer predictions (1: yes, 0: no) across the four stages, which was used to define the enhancer groups (Supplemental Experimental Procedures; Figure S2A). PU.1 and CEBPA signals were measured at the predicted enhancer groups (Supplemental Experimental Procedures; Figure S4J). Enhancer predictions were benchmarked against predictions from Lara-Astiaso et al. (2014) for activity and chromatin accessibility (see Supplemental Experimental Procedures for details).

Enrichment Analysis of Motifs

Motif enrichment was analyzed using HOMER (Heinz et al., 2010). Sequences corresponding to enhancers or regions bound by TFs were retrieved. Enrichment of TF-binding motifs, downloaded from MEME (Bailey et al., 2009), was computed for sequences of interest and for an equal number of randomly selected genomic fragments of the average region size, matched for guanine and cytosine (GC) content and autonormalized to remove bias from lower-order oligo sequences. Motif enrichment was calculated on repeat masked sequences using the cumulative binomial distribution. One hundred motifs were searched for a range of motif lengths (7–14 bp), and after filtering for redundant motifs, the top 50 motifs resulting from each search were combined, leading to a final set of motifs. These were remapped and ranked according to enrichment (depletion) in the enhancer groups.

Quantification and Statistical Analysis

ChIP-seq signals are normalized to tags per million (TPM) and are shown as the mean of the two replicates. Similarly, the mean of the three replicates of RNA-seq experiments are reported for gene expression. The statistical tests used to compute the significance level are mentioned along with the p values throughout the text.

Data and Software Availability

The accession number for the ChIP-seq and RNA-seq data reported in this paper is GEO: GSE89767.

SUPPLEMENTAL INFORMATION

Supplemental Information includes Supplemental Experimental Procedures, seven figures, and two tables and can be found with this article online at https://doi.org/10.1016/j.celrep.2018.05.012.

ACKNOWLEDGMENTS

This study was supported by the Danish Cancer Society and the NovoNordisk Foundation and through a centre grant from the NovoNordisk Foundation (Novo Nordisk Foundation Center for Stem Cell Biology, DanStem; NNF15CC0027852). E.M.S. is an EMBO Postdoctoral Fellow (ALTF 1595–2014) and is co-funded by the European Commission (LTFCOFUND2013 GA-2013-609409) and Marie Curie Actions. We thank Anna Fossum for help with cell sorting and members of the Porse lab for discussions.

AUTHOR CONTRIBUTIONS

F.K.B.L., M.B.S., J.S.J., Y.G., E.M.S., and M.S.H. performed the experiments. S.P., F.K.B.L., E.M.S., J.W., N.R., and B.T.P. analyzed the data. F.K.B.L.,

M.B.S., J.S.J., Y.G., E.M.S., M.S.H., and B.T.P. designed the experiments. S.P., F.K.B.L., and B.T.P. drafted the manuscript. All of the authors have proofread and approved the final version of the manuscript.

DECLARATION OF INTERESTS

The authors declare no competing interests.

Received: February 14, 2017
Revised: March 27, 2018
Accepted: May 3, 2018
Published: May 29, 2018

REFERENCES

Alberich-Jordà, M., Wouters, B., Balastik, M., Shapiro-Koss, C., Zhang, H., Di Ruscio, A., Radomska, H.S., Ebralidze, A.K., Amabile, G., Ye, M., et al. (2012). C/EBPγ deregulation results in differentiation arrest in acute myeloid leukemia. J. Clin. Invest. *122*, 4490–4504.

Avellino, R., Havermans, M., Erpelinck, C., Sanders, M.A., Hoogenboezem, R., van de Werken, H.J., Rombouts, E., van Lom, K., van Strien, P.M., Gebhard, C., et al. (2016). An autonomous CEBPA enhancer specific for myeloid-lineage priming and neutrophilic differentiation. Blood *127*, 2991–3003.

Bailey, T.L., Boden, M., Buske, F.A., Frith, M., Grant, C.E., Clementi, L., Ren, J., Li, W.W., and Noble, W.S. (2009). MEME SUITE: tools for motif discovery and searching. Nucleic Acids Res. *37*, W202-8.

Becker, A.M., Michael, D.G., Satpathy, A.T., Sciammas, R., Singh, H., and Bhattacharya, D. (2012). IRF-8 extinguishes neutrophil production and promotes dendritic cell lineage commitment in both myeloid and lymphoid mouse progenitors. Blood *119*, 2003–2012.

Bereshchenko, O., Mancini, E., Moore, S., Bilbao, D., Månsson, R., Luc, S., Grover, A., Jacobsen, S.E., Bryder, D., and Nerlov, C. (2009). Hematopoietic stem cell expansion precedes the generation of committed myeloid leukemia-initiating cells in C/EBPalpha mutant AML. Cancer Cell *16*, 390–400.

Boyle, A.P., Davis, S., Shulha, H.P., Meltzer, P., Margulies, E.H., Weng, Z., Furey, T.S., and Crawford, G.E. (2008). High-resolution mapping and characterization of open chromatin across the genome. Cell *132*, 311–322.

Di Stefano, B., Collombet, S., Jakobsen, J.S., Wierer, M., Sardina, J.L., Lackner, A., Stadhouders, R., Segura-Morales, C., Francesconi, M., Limone, F., et al. (2016). C/EBPα creates elite cells for iPSC reprogramming by upregulating Klf4 and increasing the levels of Lsd1 and Brd4. Nat. Cell Biol. *18*, 371–381.

Drissen, R., Buza-Vidas, N., Woll, P., Thongjuea, S., Gambardella, A., Giustacchini, A., Mancini, E., Zriwil, A., Lutteropp, M., Grover, A., et al. (2016). Distinct myeloid progenitor-differentiation pathways identified through single-cell RNA sequencing. Nat. Immunol. *17*, 666–676.

Figueroa, M.E., Wouters, B.J., Skrabanek, L., Glass, J., Li, Y., Erpelinck-Verschueren, C.A., Langerak, A.W., Löwenberg, B., Fazzari, M., Greally, J.M., et al. (2009). Genome-wide epigenetic analysis delineates a biologically distinct immature acute leukemia with myeloid/T-lymphoid features. Blood *113*, 2795–2804.

Guo, H., Cooper, S., and Friedman, A.D. (2016). In vivo deletion of the Cebpa +37 kb enhancer markedly reduces Cebpa mRNA in myeloid progenitors but not in non-hematopoietic tissues to impair granulopoiesis. PLoS One *11*, e0150809.

Hasemann, M.S., Lauridsen, F.K., Waage, J., Jakobsen, J.S., Frank, A.K., Schuster, M.B., Rapin, N., Bagger, F.O., Hoppe, P.S., Schroeder, T., and Porse, B.T. (2014). C/EBPα is required for long-term self-renewal and lineage priming of hematopoietic stem cells and for the maintenance of epigenetic configurations in multipotent progenitors. PLoS Genet. *10*, e1004079.

Heintzman, N.D., Hon, G.C., Hawkins, R.D., Kheradpour, P., Stark, A., Harp, L.F., Ye, Z., Lee, L.K., Stuart, R.K., Ching, C.W., et al. (2009). Histone modifications at human enhancers reflect global cell-type-specific gene expression. Nature *459*, 108–112.

Heinz, S., Benner, C., Spann, N., Bertolino, E., Lin, Y.C., Laslo, P., Cheng, J.X., Murre, C., Singh, H., and Glass, C.K. (2010). Simple combinations of lineage-determining transcription factors prime cis-regulatory elements required for macrophage and B cell identities. Mol. Cell *38*, 576–589.

Iwasaki, H., Somoza, C., Shigematsu, H., Duprez, E.A., Iwasaki-Arai, J., Mizuno, S., Arinobu, Y., Geary, K., Zhang, P., Dayaram, T., et al. (2005). Distinctive and indispensable roles of PU.1 in maintenance of hematopoietic stem cells and their differentiation. Blood *106*, 1590–1600.

Johansen, L.M., Iwama, A., Lodie, T.A., Sasaki, K., Felsher, D.W., Golub, T.R., and Tenen, D.G. (2001). c-Myc is a critical target for c/EBPalpha in granulopoiesis. Mol. Cell. Biol. *21*, 3789–3806.

Jones, L.C., Lin, M.L., Chen, S.S., Krug, U., Hofmann, W.K., Lee, S., Lee, Y.H., and Koeffler, H.P. (2002). Expression of C/EBPbeta from the C/ebpalpha gene locus is sufficient for normal hematopoiesis in vivo. Blood *99*, 2032–2036.

Kühn, R., Schwenk, F., Aguet, M., and Rajewsky, K. (1995). Inducible gene targeting in mice. Science *269*, 1427–1429.

Langmead, B., and Salzberg, S.L. (2012). Fast gapped-read alignment with Bowtie 2. Nat. Methods *9*, 357–359.

Lara-Astiaso, D., Weiner, A., Lorenzo-Vivas, E., Zaretsky, I., Jaitin, D.A., David, E., Keren-Shaul, H., Mildner, A., Winter, D., Jung, S., et al. (2014). Immunogenetics. Chromatin state dynamics during blood formation. Science *345*, 943–949.

Lee, Y.H., Sauer, B., Johnson, P.F., and Gonzalez, F.J. (1997). Disruption of the c/ebp alpha gene in adult mouse liver. Mol. Cell. Biol. *17*, 6014–6022.

Luyten, A., Zang, C., Liu, X.S., and Shivdasani, R.A. (2014). Active enhancers are delineated de novo during hematopoiesis, with limited lineage fidelity among specified primary blood cells. Genes Dev. *28*, 1827–1839.

Madsen, M.S., Siersbæk, R., Boergesen, M., Nielsen, R., and Mandrup, S. (2014). Peroxisome proliferator-activated receptor γ and C/EBPα synergistically activate key metabolic adipocyte genes by assisted loading. Mol. Cell. Biol. *34*, 939–954.

Mancini, E., Sanjuan-Pla, A., Luciani, L., Moore, S., Grover, A., Zay, A., Rasmussen, K.D., Luc, S., Bilbao, D., O'Carroll, D., et al. (2012). FOG-1 and GATA-1 act sequentially to specify definitive megakaryocytic and erythroid progenitors. EMBO J. *31*, 351–365.

Ohlsson, E., Schuster, M.B., Hasemann, M., and Porse, B.T. (2016). The multifaceted functions of C/EBPα in normal and malignant haematopoiesis. Leukemia *30*, 767–775.

Olsson, A., Venkatasubramanian, M., Chaudhri, V.K., Aronow, B.J., Salomonis, N., Singh, H., and Grimes, H.L. (2016). Single-cell analysis of mixed-lineage states leading to a binary cell fate choice. Nature *537*, 698–702.

Orkin, S.H., and Zon, L.I. (2008). Hematopoiesis: an evolving paradigm for stem cell biology. Cell *132*, 631–644.

Paul, F., Arkin, Y., Giladi, A., Jaitin, D.A., Kenigsberg, E., Keren-Shaul, H., Winter, D., Lara-Astiaso, D., Gury, M., Weiner, A., et al. (2015). Transcriptional heterogeneity and lineage commitment in myeloid progenitors. Cell *163*, 1663–1677.

Porse, B.T., Pedersen, T.A., Xu, X., Lindberg, B., Wewer, U.M., Friis-Hansen, L., and Nerlov, C. (2001). E2F repression by C/EBPalpha is required for adipogenesis and granulopoiesis in vivo. Cell *107*, 247–258.

Pundhir, S., Bagger, F.O., Lauridsen, F.B., Rapin, N., and Porse, B.T. (2016). Peak-valley-peak pattern of histone modifications delineates active regulatory elements and their directionality. Nucleic Acids Res. *44*, 4037–4051.

Rosenbauer, F., and Tenen, D.G. (2007). Transcription factors in myeloid development: balancing differentiation with transformation. Nat. Rev. Immunol. *7*, 105–117.

Rosenbauer, F., Wagner, K., Kutok, J.L., Iwasaki, H., Le Beau, M.M., Okuno, Y., Akashi, K., Fiering, S., and Tenen, D.G. (2004). Acute myeloid leukemia induced by graded reduction of a lineage-specific transcription factor, PU.1. Nat. Genet. *36*, 624–630.

Schuster, M.B., Frank, A.K., Bagger, F.O., Rapin, N., Vikesaa, J., and Porse, B.T. (2013). Lack of the p42 form of C/EBPalpha leads to spontaneous immortalization and lineage infidelity of committed myeloid progenitors. Exp. Hematol. *41*, 882–893.e16.

Scott, E.W., Simon, M.C., Anastasi, J., and Singh, H. (1994). Requirement of transcription factor PU.1 in the development of multiple hematopoietic lineages. Science *265*, 1573–1577.

Wagner, K., Zhang, P., Rosenbauer, F., Drescher, B., Kobayashi, S., Radomska, H.S., Kutok, J.L., Gilliland, D.G., Krauter, J., and Tenen, D.G. (2006). Absence of the transcription factor CCAAT enhancer binding protein alpha results in loss of myeloid identity in bcr/abl-induced malignancy. Proc. Natl. Acad. Sci. USA *103*, 6338–6343.

Wilson, N.K., Foster, S.D., Wang, X., Knezevic, K., Schütte, J., Kaimakis, P., Chilarska, P.M., Kinston, S., Ouwehand, W.H., Dzierzak, E., et al. (2010). Combinatorial transcriptional control in blood stem/progenitor cells: genome-wide analysis of ten major transcriptional regulators. Cell Stem Cell *7*, 532–544.

Wouters, B.J., Jordà, M.A., Keeshan, K., Louwers, I., Erpelinck-Verschueren, C.A., Tielemans, D., Langerak, A.W., He, Y., Yashiro-Ohtani, Y., Zhang, P., et al. (2007). Distinct gene expression profiles of acute myeloid/T-lymphoid leukemia with silenced CEBPA and mutations in NOTCH1. Blood *110*, 3706–3714.

Yeamans, C., Wang, D., Paz-Priel, I., Torbett, B.E., Tenen, D.G., and Friedman, A.D. (2007). C/EBPalpha binds and activates the PU.1 distal enhancer to induce monocyte lineage commitment. Blood *110*, 3136–3142.

Zhang, P., Iwasaki-Arai, J., Iwasaki, H., Fenyus, M.L., Dayaram, T., Owens, B.M., Shigematsu, H., Levantini, E., Huettner, C.S., Lekstrom-Himes, J.A., et al. (2004). Enhancement of hematopoietic stem cell repopulating capacity and self-renewal in the absence of the transcription factor C/EBP alpha. Immunity *21*, 853–863.

Zhang, H., Alberich-Jorda, M., Amabile, G., Yang, H., Staber, P.B., Di Ruscio, A., Welner, R.S., Ebralidze, A., Zhang, J., Levantini, E., et al. (2013). Sox4 is a key oncogenic target in C/EBPα mutant acute myeloid leukemia. Cancer Cell *24*, 575–588.